

Supporting Information

Progressively Stimulating Carrier Motion Over Transient Metal Chalcogenides Quantum Dots Towards Solar-to-Hydrogen Conversion

Shi-Cheng Zhu^a, Zi-Chen Wang^a, Bo Tang^a, Hao Liang^a, Bi-Jian Liu^a, Shen Li^a, Zhixin Chen, Nian-Cai
Cheng^a, Fang-Xing Xiao^{*ab}

a. College of Materials Science and Engineering, Fuzhou University, New Campus, Minhou,

Fujian Province, 350108, China.

b. Fujian Science & Technology Innovation Laboratory for Optoelectronic Information of China,

Fuzhou, Fujian 350108, China.

c. Instrumental Measurement and Analysis Center, Fuzhou University, Fuzhou, 350108, China.

E-mail: fx Xiao@fzu.edu.cn

Table of Contents

Page NO.

Experimental section	S3
Figure S1. XRD, FESEM image, UV-vis, zeta potential, AFM and the corresponding height profile of $Ti_3C_2T_x$	S6
Figure S2. HRTEM image, size distribution histogram, zeta potential, UV-vis absorption spectra of CdSe and CdSe:2Ni.....	S7
Figure S3. EDX result of CdSe QDs:2Ni-MNs hybrids.....	S8
Figure S4. Zeta potential, UV-vis absorption spectrum of CdS QDs & CdSe QDs:2Ni and CdTe QDs & CdTe QDs:2Ni	S9
Figure S5. XRD pattern of CdS QDs:2Ni-MNs and CdTe QDs:2Ni-MNs.....	S10
Figure S6. FTIR spectra of CdS QDs:2Ni-MNs and CdTe QDs:2Ni-MNs.....	S11
Figure S7. Survey spectra and high-resolution of CdSe QDs:2Ni-MNs hybrids.....	S12
Figure S8. DRS results of CdS QDs:2Ni-MNs and CdTe QDs:2Ni-MNs.....	S13
Figure S9. Photocatalytic H_2 evolution of CdSe QDs:2Ni-MNs under different light intensity.....	S14
Figure S10. Calculated charge density difference for CdSe QDs:2Ni.....	S15
Figure S11. Charge carrier density of CdSe QDs, CdSe QDs:2Ni, and CdSe QDs:2Ni-MNs heterostructure.....	S16
Figure S12. Mott-Schottky plots of CdSe QDs and CdSe QDs:2Ni probed under different frequencies.....	S17
Figure S13. VB XPS spectrums of CdSe QDs and CdSe QDs:2Ni.....	S18
Table S1. Bandgaps of the six samples.....	S19
Table S2. Chemical bond species vs. B.E. for the three samples.....	S20
Table S3. Peak position with corresponding functional groups.....	S21
Table S4. Summary of specific surface area, pore volume and pore size of the two samples.....	S22
Table S5. Solar-to-hydrogen conversion efficiency (S.T.H) of CdSe QDs:2Ni-MNs.....	S23
Table S6. Apparent Quantum efficiency (AQE) of CdSe QDs:2Ni-MNs.....	S24
References	S25

1. Experimental section

1.1 Materials

Cadmium chloride ($\text{CdCl}_2 \cdot 2.5\text{H}_2\text{O}$), selenium (Se) powder, tellurium (Te) powder, sodium borohydride (NaBH_4), 2-aminoethanethiol (AET), hydrochloric acid (HCl), lithium fluoride (LiF), methanol (CH_4O), ethanol ($\text{C}_2\text{H}_6\text{O}$), ethylene glycol ($\text{C}_2\text{H}_6\text{O}_2$), glycerol ($\text{C}_3\text{H}_8\text{O}_3$), triethanolamine ($\text{C}_6\text{H}_{15}\text{NO}_3$), calcium chloride (CaCl_2), cobaltous chloride (CoCl_2), chromium chloride hexahydrate ($\text{CrCl}_3 \cdot 6\text{H}_2\text{O}$), cupric chloride (CuCl_2), manganese(II) chloride (MnCl_2), ferrous chloride (FeCl_2), nickel chloride (NiCl_2), sodium sulfite (Na_2SO_3), sodium sulfide (Na_2S), sodium sulfate (Na_2SO_4), deionized water (DI H_2O , Millipore, 18.2 $\text{M}\Omega$ cm resistivity) are used. Ti_3AlC_2 powder was obtained from Laizhou Kai Kai Ceramic Materials Co., Ltd. All the materials are of analytical grade and used as received without further purification.

1.2 Preparation of positively charged CdSe QDs

Specifically, 2 mmol $\text{CdCl}_2 \cdot 2.5\text{H}_2\text{O}$ was dissolved in 200 mL of deionized water in a three-necked flask and deaerated with N_2 bubbling for 1 h. 250 mg of AET as a stabilizer was then added to the above solution. The pH value of the solution was adjusted to 5 with 1 M HCl aqueous solution. Subsequently, oxygen-free NaHSe solution was prepared by mixing 0.2106 g of Se powder and 0.6320 g NaBH_4 into 10 mL of deionized water under N_2 bubbling and ice bath for 2 h. Then, 5 mL of freshly prepared oxygen-free NaHSe solution was quickly injected into the N_2 saturated Cd^{2+} solution under vigorous stirring. The initial molar ratio of Cd^{2+} : Se^{2-} : AET was 3: 2: 5. After refluxing at 80 °C for 4 h, the desired yellow CdSe QDs solution was obtained. To purify the as-prepared CdSe QDs, equal volume of ethanol was added into the above solution to precipitate CdSe QDs. The precipitated CdSe QDs was separated by centrifugation, further washed with water and ethanol for several times, and dried in vacuum at 60 °C.¹

1.3 Preparation of positively charged CdS QDs

Briefly, 250 mg of AET was added to 200 mL of CdCl_2 (0.01 M) aqueous solution, and N_2 was bubbled throughout the solution to remove O_2 at 110 °C. During this period, 1.0 M HCl aqueous solution was slowly added to adjust the solution pH to 5. Following, 22 mL of 0.1 M Na_2S aqueous solution was injected to grow the AET-capped water soluble CdS QDs. The reaction mixture was refluxed under N_2 atmosphere for 4 h. To purify the as-prepared CdS QDs, equal volume of ethanol was added into the above solution to precipitate CdS QDs. The precipitated CdS QDs was separated by centrifugation, further washed with water and ethanol for several times, and dried in vacuum at 60 °C.²

1.4 Preparation of positively charged CdS QDs:2Ni

On the basis of **1.3 Preparation of positively charged CdS QDs**, 400 μL of NiCl_2 aqueous solution (0.1 M) needs to be added into 200 mL CdCl_2 (0.01 M) solution first, and other process steps remain unchanged.

1.5 Preparation of positively charged CdTe QDs

CdTe QDs were synthesized by a previously method. Specifically, 2 mmol of $\text{CdCl}_2 \cdot 2.5\text{H}_2\text{O}$ was dissolved in 200 mL of DI H_2O and deaerated with N_2 bubbling in a three-necked flask for 1 h. After that, 250 mg of AET as a stabilizer was added into the above solution and pH value of the mixture was carefully adjusted to 5 with 1 M HCl aqueous solution. Subsequently, oxygen-free NaHTe aqueous solution was prepared by dissolving 1.2640 g of NaBH_4 in 10 mL of DI H_2O under N_2 bubbling, into which 0.3403 g of Te powder was added and stirred at a low speed for 2 h in an ice bath. 5 mL of the freshly prepared NaHTe aqueous solution was then quickly injected into Cd^{2+} aqueous solution under vigorous stirring and a red solution was obtained and then it was refluxed in 333 K for 4 h. After cooling to room temperature, CdTe QDs aqueous solution was precipitated by adding into equal volume of ethanol with vigorous stirring and the precipitate was separated by centrifugation and dried in vacuum at 313 K.³

1.6 Preparation of positively charged CdTe QDs:2Ni

On the basis of **1.5 Preparation of positively charged CdTe QDs**, 400 μL of NiCl_2 aqueous solution (0.1 M) needs to be added into 200 mL CdCl_2 (0.01 M) solution first, and other process steps remain unchanged.

1.7 Preparation of $\text{Ti}_3\text{C}_2\text{T}_x$ (MXene)

$\text{Ti}_3\text{C}_2\text{T}_x$ (MXene) colloid was prepared as described previously. In detail, multilayered $\text{Ti}_3\text{C}_2\text{T}_x$ was firstly synthesized by etching 1g Ti_3AlC_2 powders in a mixture of 1g lithium fluoride and 10 mL hydrochloric acid (9 mol L^{-1}) for 24h at 35 $^\circ\text{C}$. The product was washed with deionized water until the pH of the supernatant was above 5. The multilayered $\text{Ti}_3\text{C}_2\text{T}_x$ powder was then added into 200 mL deionized water and delaminated by bath sonication for 1h under N_2 flow. After centrifugation for 1h at 3500 rpm, the dark green supernatant was collected. The concentration of the delaminated $\text{Ti}_3\text{C}_2\text{T}_x$ was determined by filtering a known volume of the supernatant through a Celgard membrane and measuring the weight of the film after drying.⁴

1.8 Photoelectrochemical (PEC) measurements

PEC measurements were carried out on an electrochemical workstation (CHI660E, CHI Shanghai, Inc.) with conventional three-electrode system and 0.5 M Na₂SO₄ aqueous solution (pH=6.69) was utilized as the electrolyte.⁵ The three-electrode system is composed of Pt foil (1 cm × 1 cm) which was used as the counter electrode and Ag/AgCl electrode as the reference electrode, and the working electrodes were prepared on fluorine-doped tin oxide (FTO) glass that was cleaned by sonication in DI H₂O and ethanol for 30 min and dried at 333 K in an oven. The boundary of FTO glass was protected using Scotch tape. Specifically, 10 mg of the sample was dispersed in 0.5 mL of ethanol by sonication to get slurry which was spread onto the pretreated FTO glass.⁶ After air drying, the Scotch tape was unstuck and the uncoated part of the electrode was isolated with nail polish. The exposed area of the working electrode was 1 cm². Finally, the working electrode was vertically dipped into the electrolyte and irradiated with visible light ($\lambda > 420$ nm) (PLS-SXE300D, Beijing Perfect Light Co. Ltd., China). Potentials of the electrode were calibrated against the reversible hydrogen electrode (RHE) based on the following **Formula**:

$$E_{\text{RHE}} = E_{\text{Ag/AgCl}} + 0.059\text{pH} + E^{\circ}_{\text{Ag/AgCl}} \quad (E^{\circ}_{\text{Ag/AgCl}} = 0.1976 \text{ V at } 25 \text{ }^{\circ}\text{C}) \quad (\text{S1})$$

Transient photocurrent response (i.e., I-t) was collected under chopped light irradiation (light on/off cycle: 30 s) at a fixed bias of 1.23 V vs. RHE. Electrochemical impedance spectra (EIS) were measured on an electrochemical workstation (IM6, Zahner Germany) with an amplitude of 10 mV in the frequency ranging from 10⁵ to 0.1 Hz.

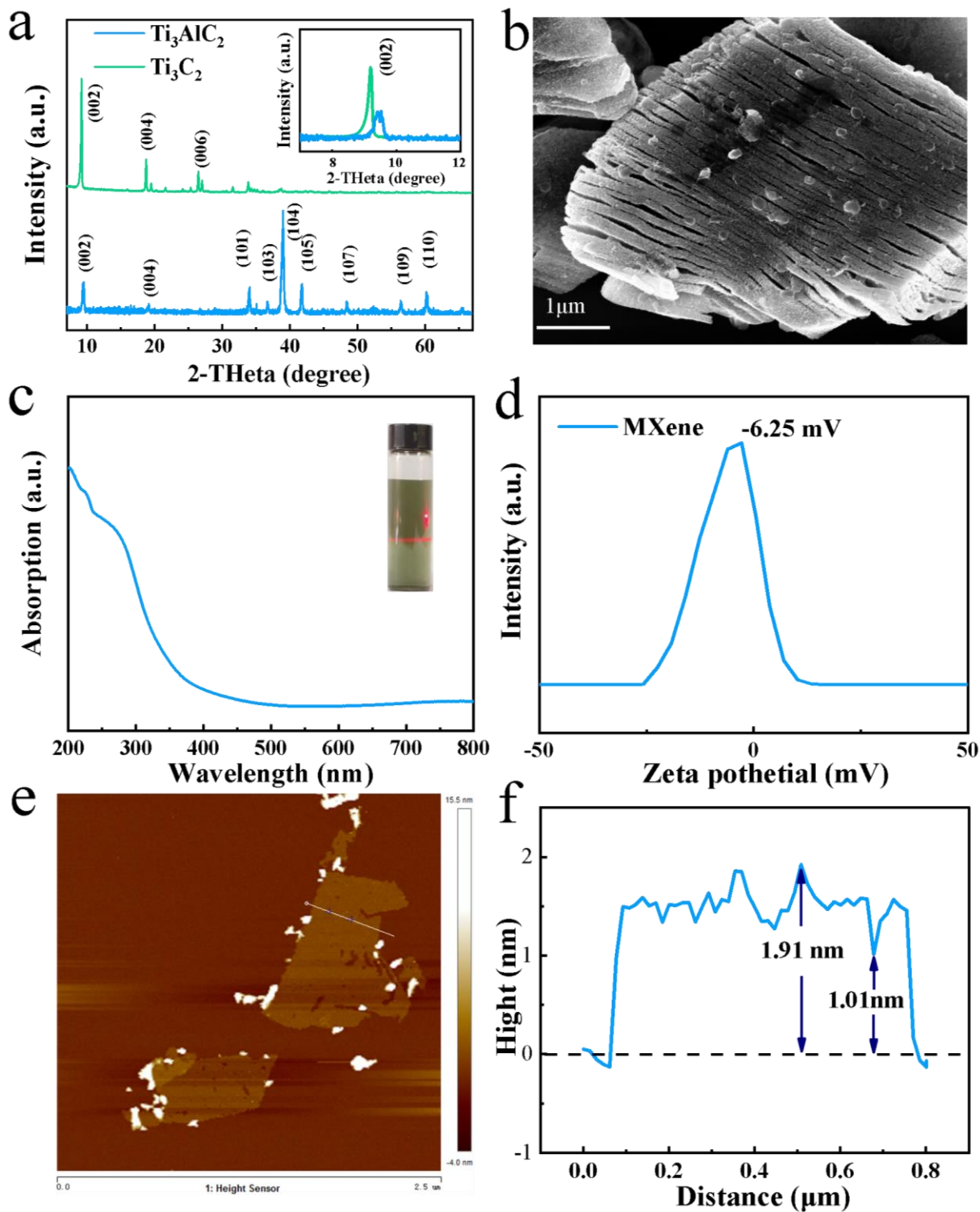


Fig. S1. (a) XRD patterns, (b) FESEM image after etching, (c) UV-vis absorption spectrum with photographs in the inset, (d) zeta potential (pH=7), (e) AFM image and (f) height profile of $Ti_3C_2T_x$ MNs.

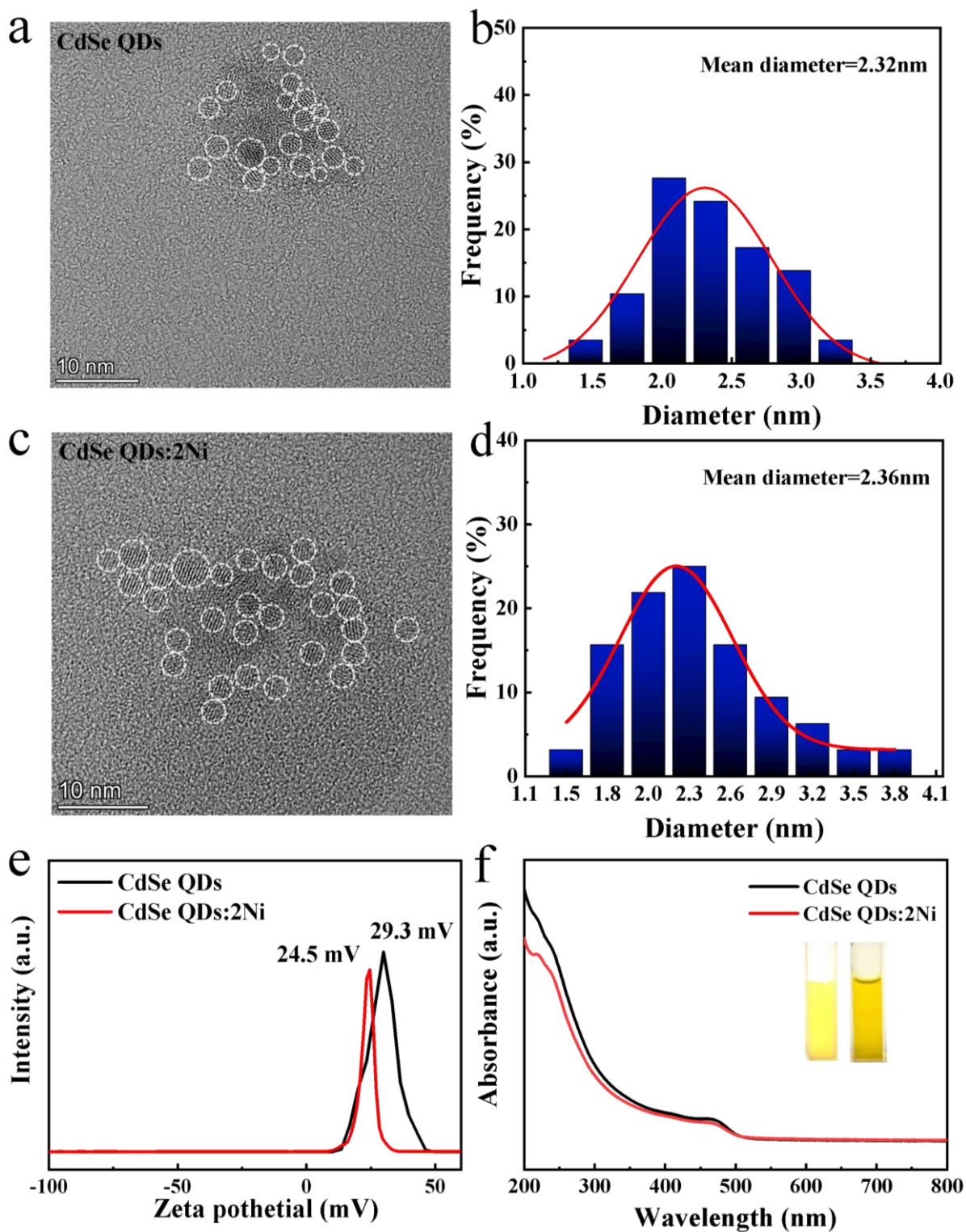


Fig. S2. (a & c) HRTEM images, (b & d) size distribution histograms, and (e) zeta potentials (pH=7) of CdSe QDs and CdSe QDs:2Ni. (f) UV-vis absorption spectra of CdSe QDs & CdSe QDs:2Ni colloidal aqueous solutions with photographs in the inset.

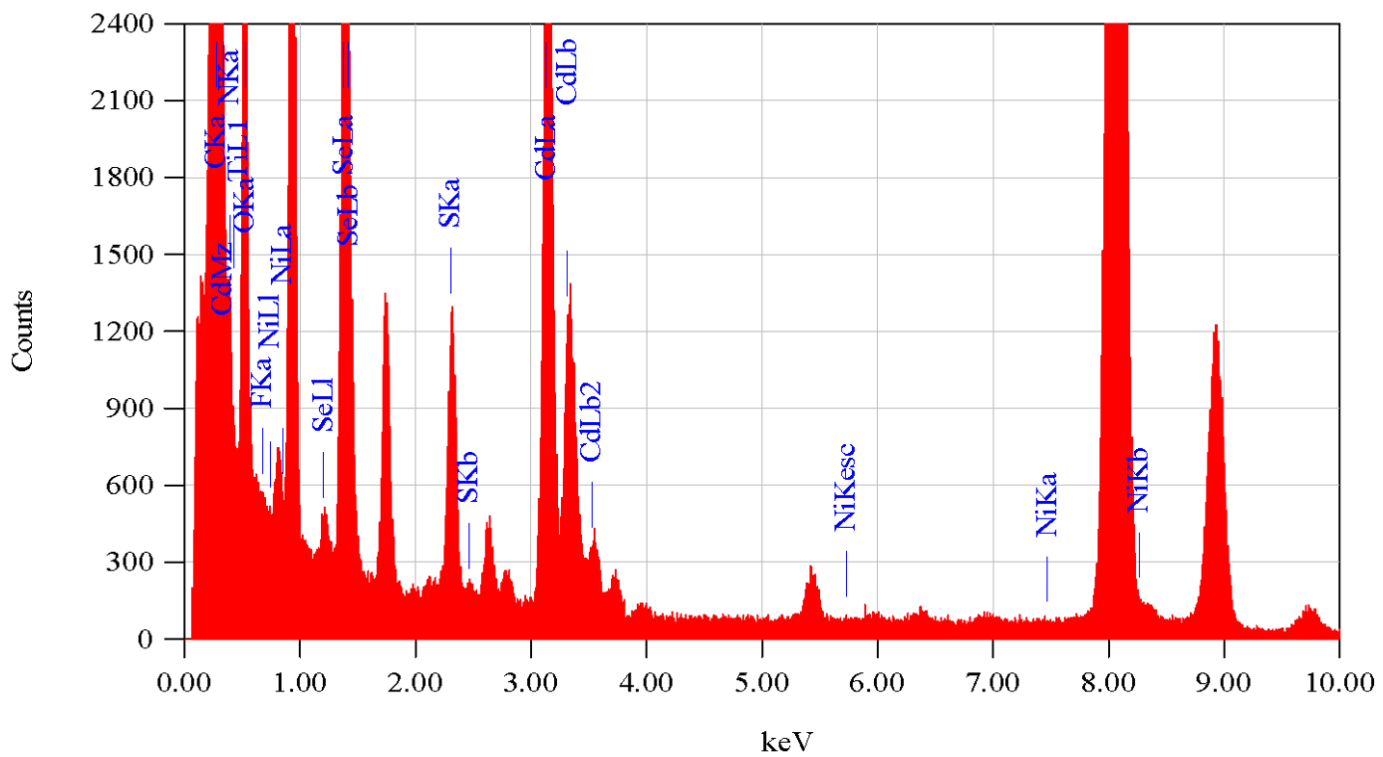


Fig. S3. EDX result of CdSe QDs:2Ni-MNs.

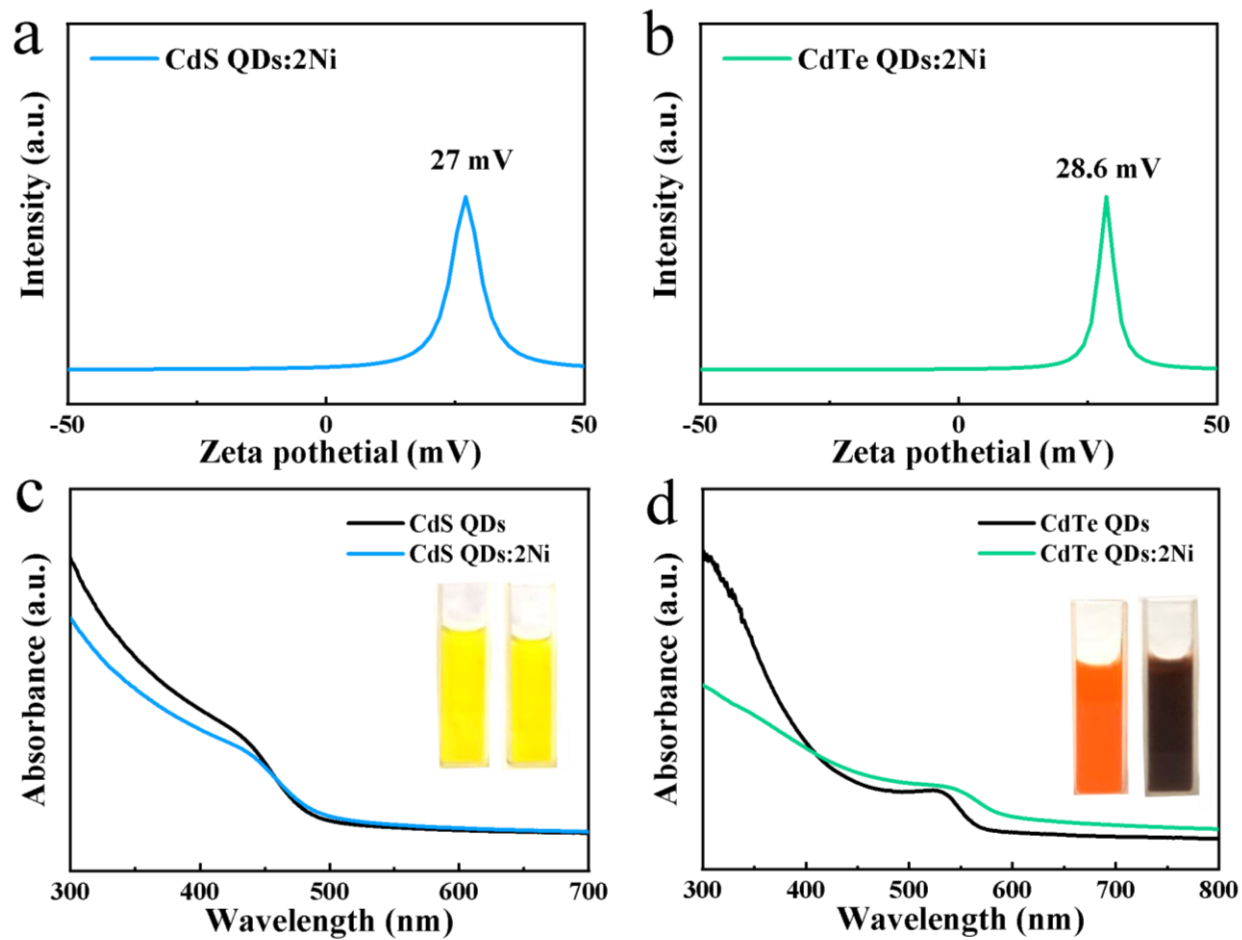


Fig. S4. Zeta potentials (pH=7) of (a) CdS QDs:2Ni and (b) CdTe QD:2Ni. UV-vis absorption spectra of (c) CdS QDs & CdS QDs:2Ni and (d) CdTe QDs & CdTe QDs:2Ni.

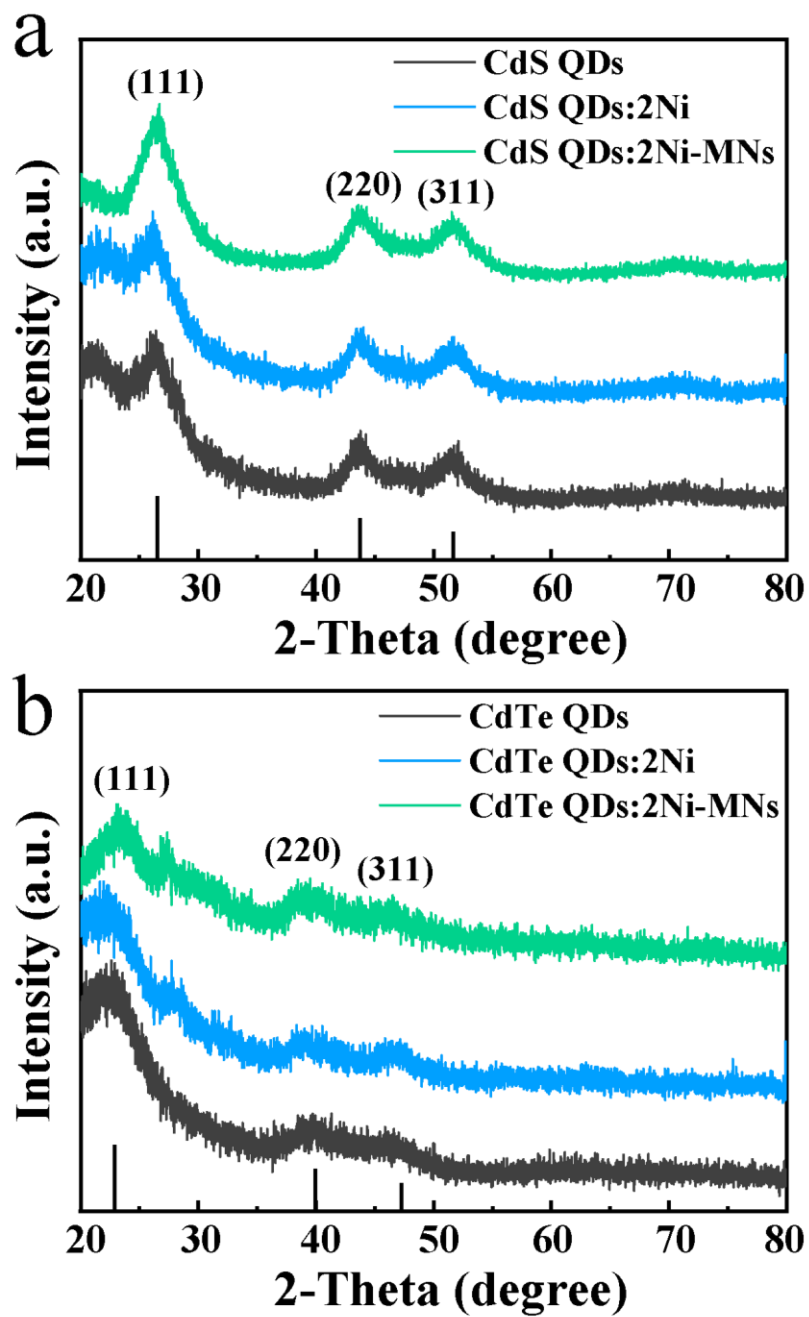


Fig. S5. XRD patterns of (a) CdS QDs, CdS QDs:2Ni, and CdS QDs:2Ni-MNs; (b) XRD patterns of CdTe QDs, CdTe QDs:2Ni, and CdTe QDs:2Ni-MNs.

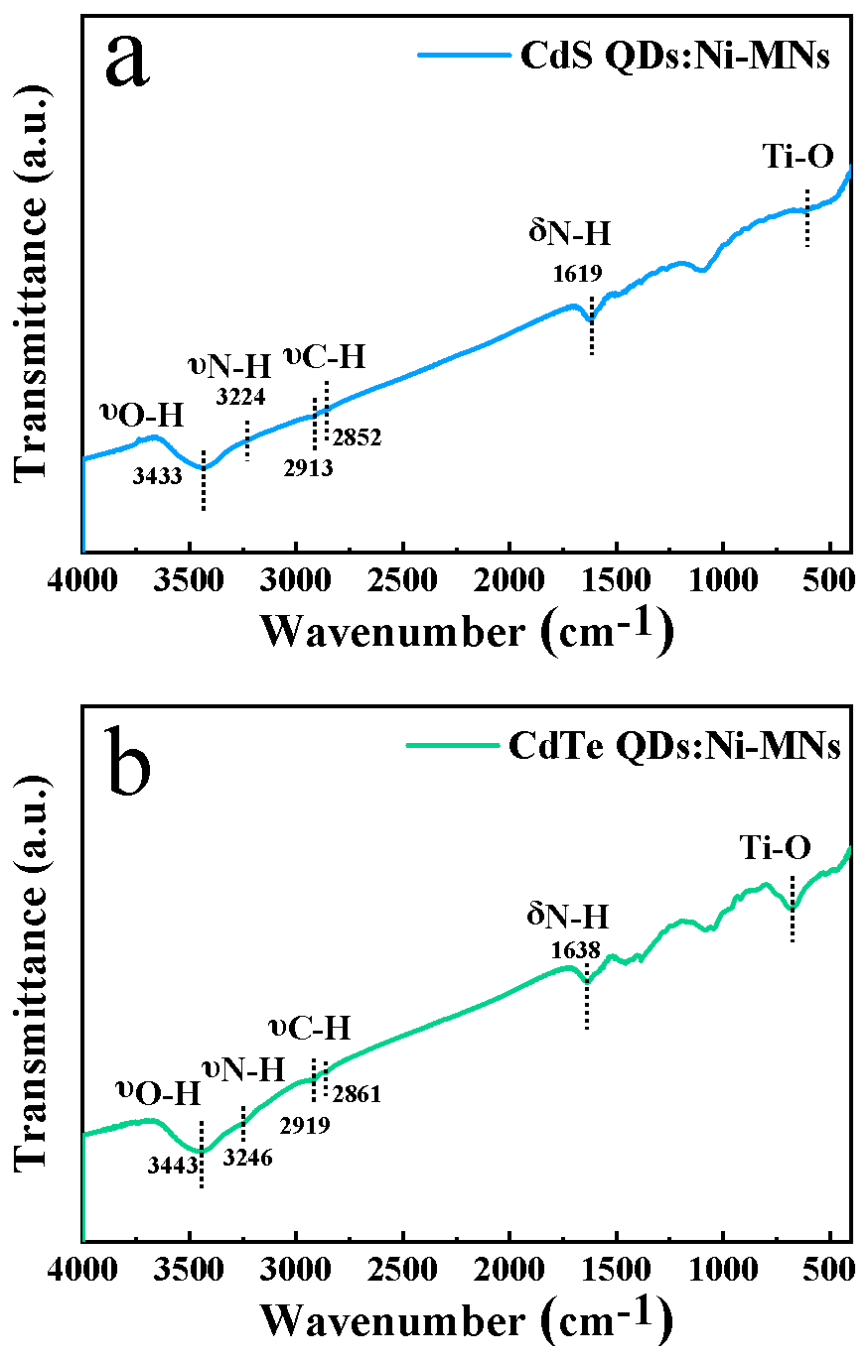


Fig. S6. FTIR spectra of (a) CdS QDs:2Ni-MNs and (b) CdTe QDs:2Ni-MNs

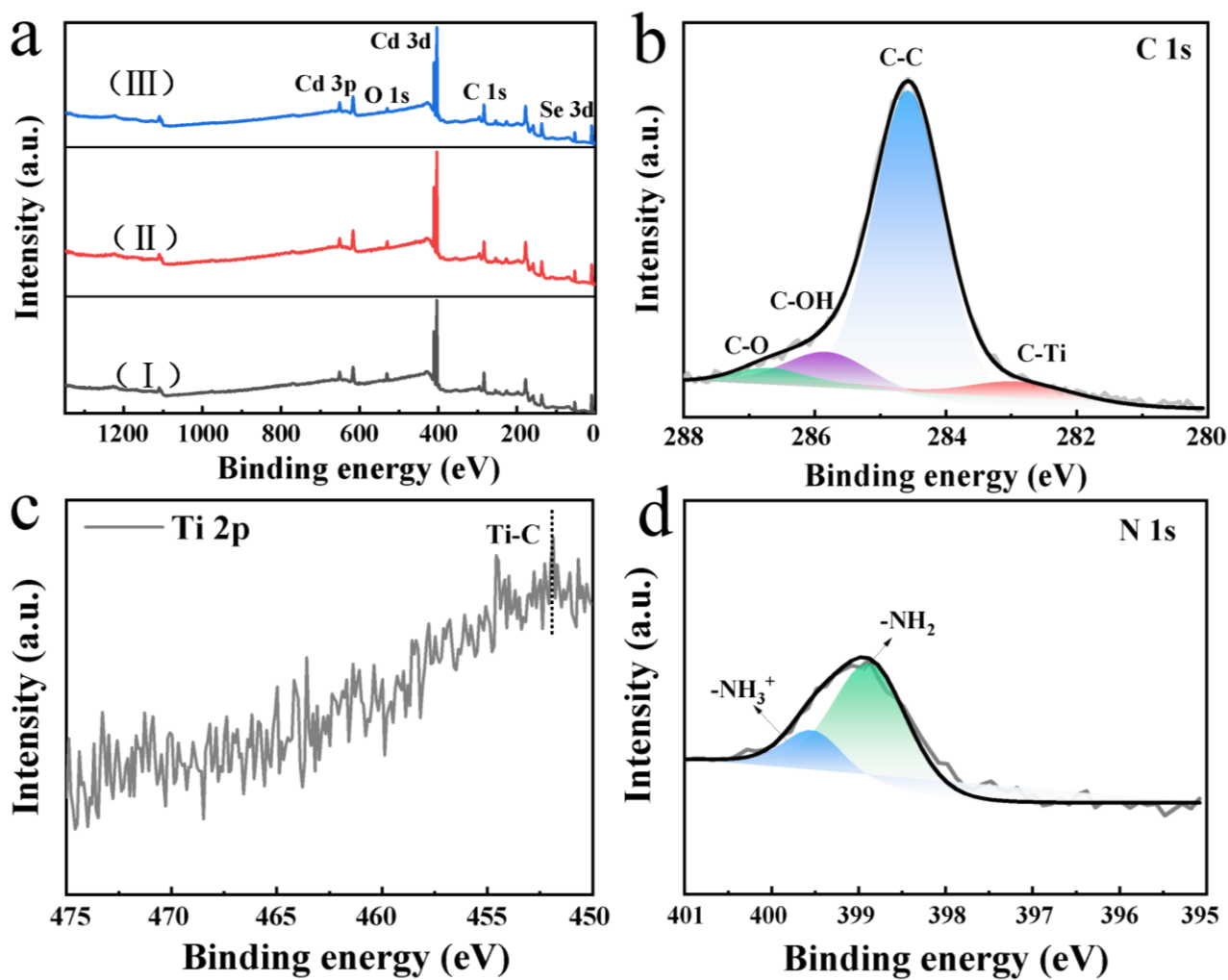


Fig. S7. (a) Survey spectra of (I) CdSe QDs, (II) CdSe QDs:2Ni, and (III) CdSe QDs:2Ni-MNs; high-resolution spectra of (b) C 1s, (c) Ti 2p, and (d) N 1s for CdSe QDs:2Ni-MNs.

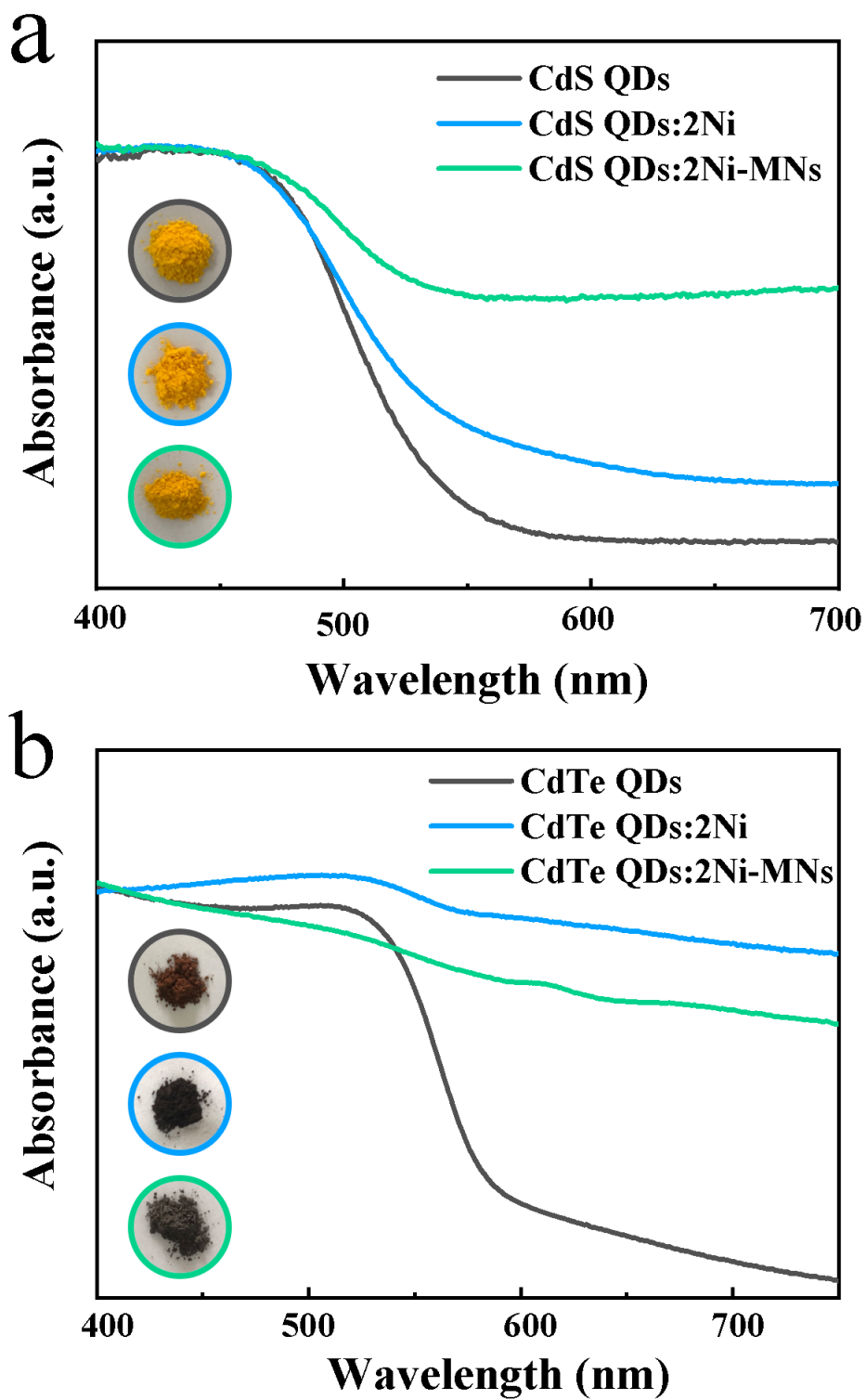


Fig. S8. DRS results of (a) CdS QDs, CdS QDs:2Ni, and CdS QDs:2Ni-MNs; (b) DRS results of CdTe QDs, CdTe QDs:2Ni, and CdTe QDs:2Ni-MNs with photographs in the inset.

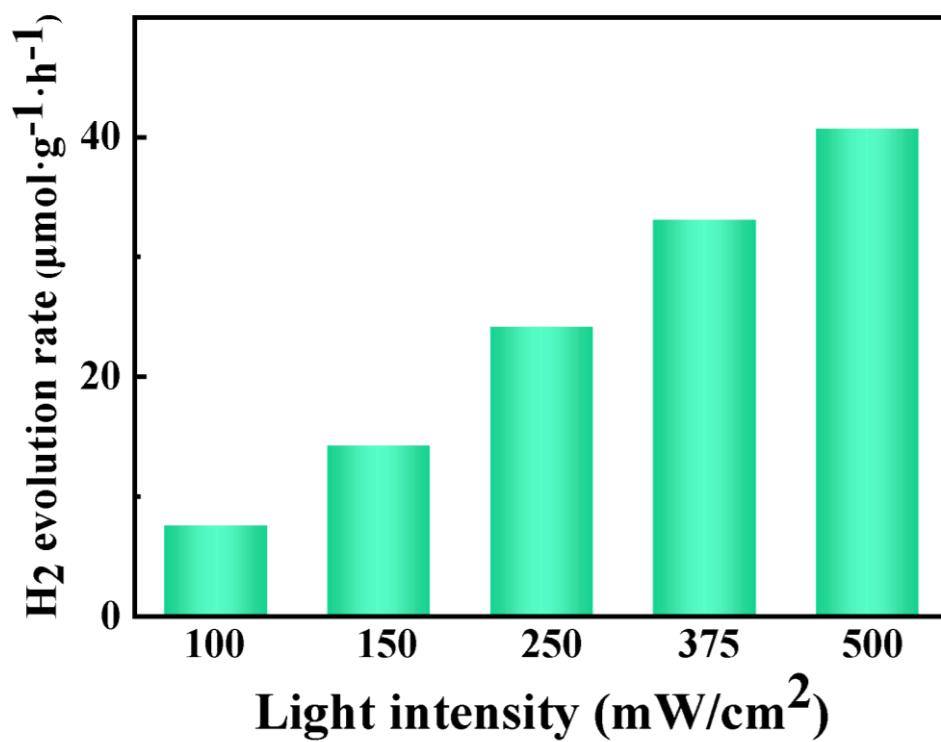


Fig. S9. Photocatalytic hydrogen production performances of CdSe QDs:2Ni-MNs under visible light irradiation with different light intensity.

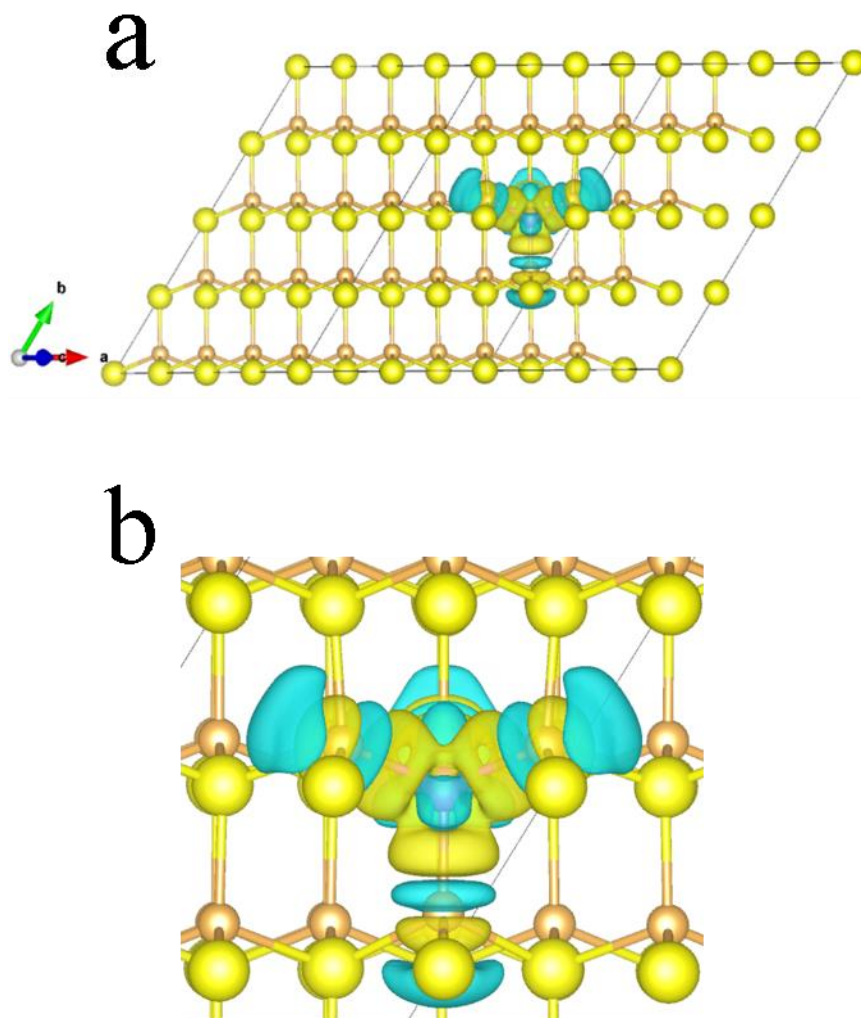


Fig. S10. Calculated charge density difference for CdSe QDs:2Ni. Cyan bubbles mean charge depletion and yellow bubbles represent charge accumulation.

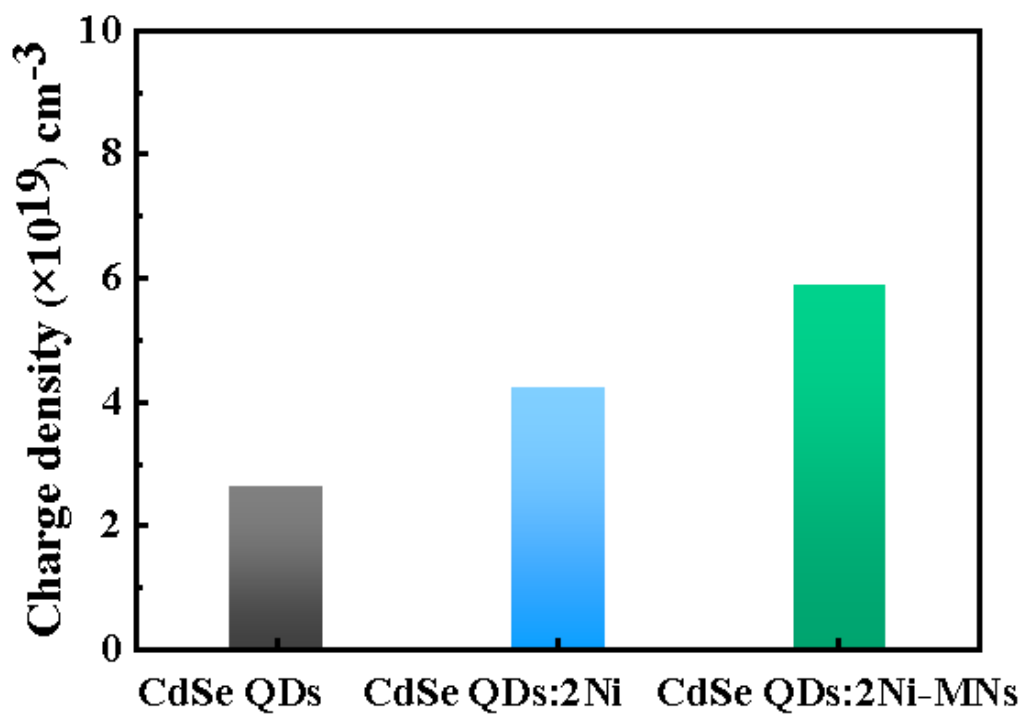


Fig. S11. Charge carrier density (ND) of CdSe QDs, CdSe QDs:2Ni, and CdSe QDs:2Ni-MNs.

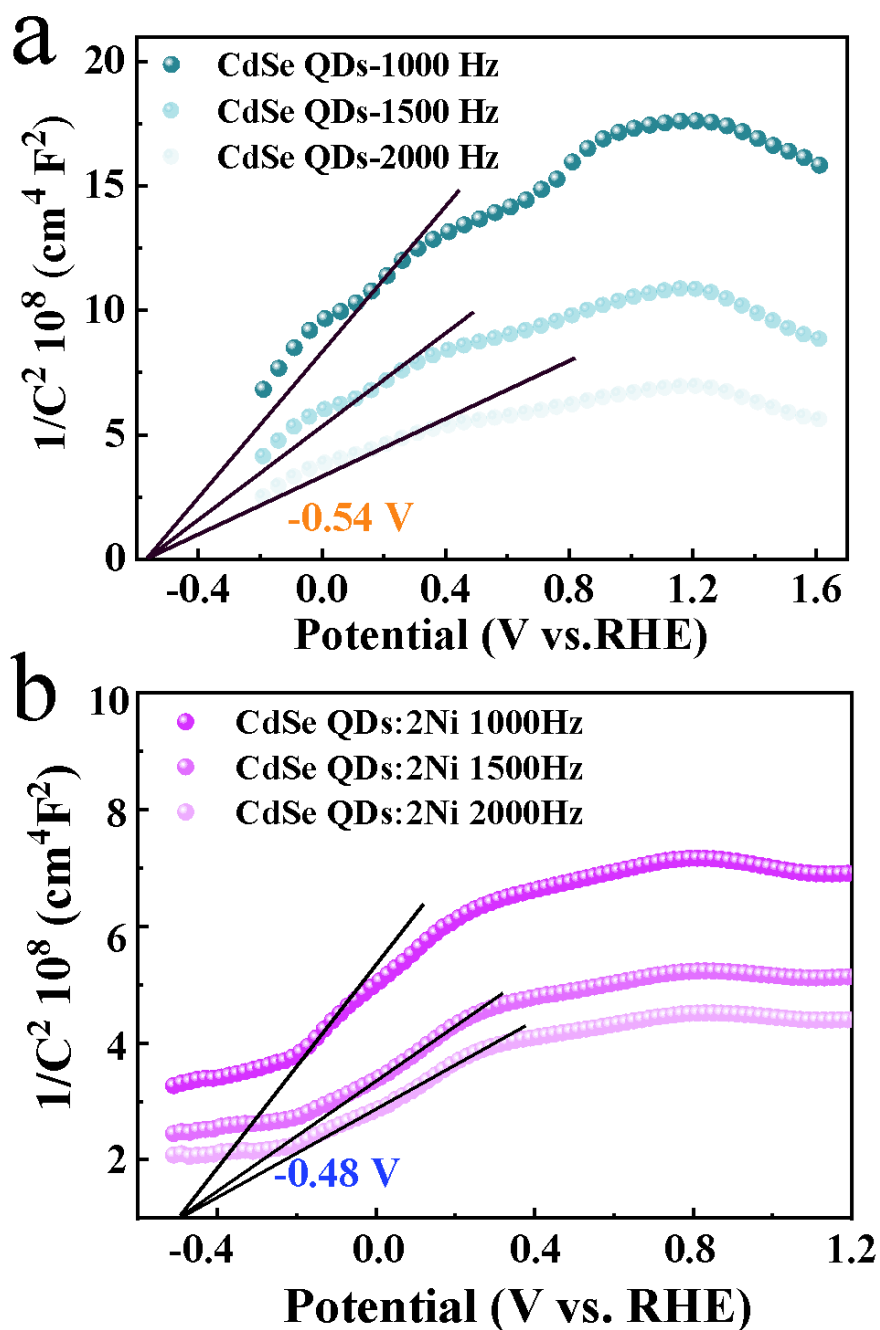


Fig. S12. Mott-Schottky plots of CdSe QDs and CdSe QDs:2Ni probed under different frequency.

Note: Flat band position (V_{fb}) can be determined by Mott-Schottky plots probed under different frequencies. Apparently, intersection point does not depend on the frequency and V_{fb} of CdSe QDs:2Ni is approximately determined as -0.48 V vs. RHE (-0.87 V vs. NHE).

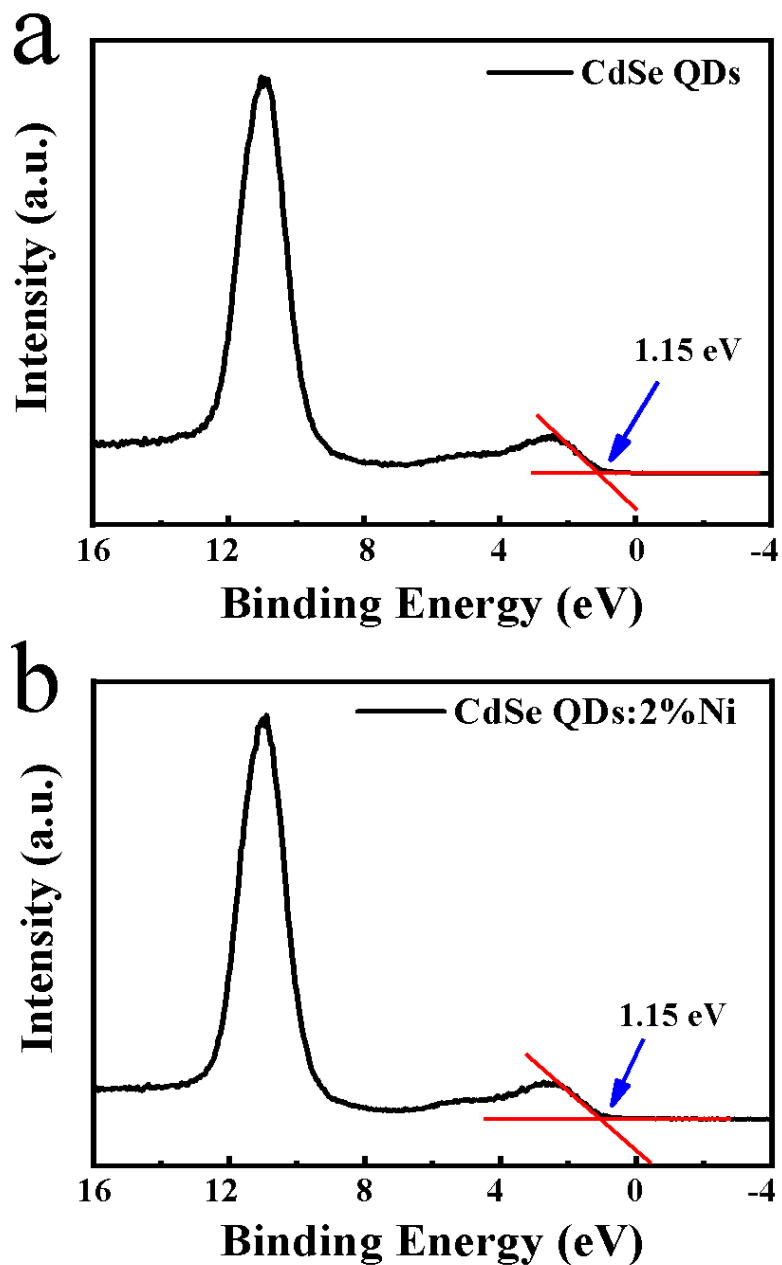


Fig. S13. VB XPS spectra of (a) CdSe QDs and (b) CdSe QDs:2Ni.

Table S1. Peak position with corresponding functional groups.

<i>Peak position (cm⁻¹)</i>	<i>Vibrational mode</i>	<i>Functional groups/Ingredient</i>
3433	<i>ν_{O-H}</i>	<i>-OH & -COOH/H₂O</i>
3223	<i>ν_{N-H}</i>	<i>-NH₂/AET</i>
2919 & 2853	<i>ν_{C-H}</i>	<i>-CH₂/AET</i>
1636	<i>δ_{O-H}</i>	<i>-OH</i>
1572	<i>δ_{N-H}</i>	<i>-NH₂/AET</i>
548	<i>Ti-O</i>	<i>Ti-O/MXene^{S7}</i>

Table S2. Chemical bond species vs. B.E. for different samples.

<i>Elements</i>	<i>CdSe QDs</i>	<i>CdSe QDs:2Ni</i>	<i>CdSe QDs:2Ni-MNs</i>	<i>Chemical Bond Species</i>
Cd 3d_{5/2}	403.81	403.81	403.94	Cd ²⁺
Cd 3d_{3/2}	410.57	410.57	410.72	Cd ²⁺
Se 3d_{5/2}	53.60	53.60	53.85	Se ²⁻
Se 3d_{3/2}	54.47	54.47	54.83	Se ²⁻
Ni 2p_{3/2}	N.D.	N.D.	N.D.	Ni ²⁺
Ni 2p_{1/2}	N.D.	874.2	874.2	Ni ²⁺ S8
C 1s A	284.80	284.80	284.80	C-C
C 1s B	N.D.	N.D.	282.53	C-Ti S9
C 1s C	N.D.	N.D.	285.90	C-OH
C 1s D	N.D.	N.D.	286.78	C-O S10
Ti 2p	N.D.	N.D.	452.03	Ti-C S11
N 1s A	398.89	398.89	398.89	-NH ₂ S12
N 1s B	399.57	399.57	399.57	-NH ³⁺

N.D.: Not Detected.

Table S3. Bandgaps of CdSe QDs:Ni (0%, 0.5%,1.0%, 2.0%, 4%) and CdSe QDs:2Ni-MNs.

<i>Samples</i>	<i>Bandgap (eV)</i>
CdSe QDs	2.17
CdSe QDs:0.5Ni	2.15
CdSe QDs:1.0Ni	2.13
CdSe QDs:2.0Ni	2.05
CdSe QDs:4.0Ni	1.95
CdSe QDs:2.0Ni-MNs	1.86

Table S4. Specific surface areas and pore size of different samples.

<i>Samples</i>	<i>S_{BET} (m² g⁻¹)^a</i>	<i>Pore volume (cm³ g⁻¹)^b</i>	<i>Pore size (Å)^c</i>
CdSe QDs:2Ni	72.1025	0.237030	131.4908
CdSe QDs:2Ni-MNs	75.3670	0.140841	74.7492

^a BET surface area is calculated from the linear part of BET plots.

^b Single point total pore volume of the pores at P/P0 = 0.99.

^c Adsorption average pore width (4V/A by BET).

Table S5. S.T.H. efficiency of CdSe QDs:2Ni-MNs, CdSe QDs:2Ni and pristine CdSe QDs.

<i>Photocatalyst</i>	<i>Light source</i>	<i>Activity (mmol h⁻¹ g⁻¹)</i>	<i>S.T.H (%)</i>
CdSe QDs:2Ni-MNs	420 nm	4.12	20.8
	450 nm	5.80	29.3
	500 nm	9.44	47.7
	550 nm	5.66	28.6
	600 nm	0.47	2.4
	650 nm	0	0
	700 nm	0	0
CdSe QDs:2Ni	500 nm	6.21	31.4
CdSe QDs	500 nm	0.43	2.2

Table S6. AQE of CdSe QDs:2Ni-MNs, CdSe QDs:2Ni and pristine CdSe QDs.

<i>Photocatalyst</i>	<i>Light source</i>	<i>Activity ($\mu\text{mol h}^{-1}$)</i>	<i>AQE (%)</i>
CdSe QDs:2Ni-MNs	420 nm	41.2	0.435
	450 nm	58.0	0.572
	500 nm	94.4	0.838
	550 nm	56.6	0.457
	600 nm	4.7	0.035
	650 nm	0	0
	700 nm	0	0
CdSe QDs:2Ni	500 nm	62.1	0.551
CdSe QDs	500 nm	4.3	0.038

References

1. M.-H. Huang, X.-C. Dai, T. Li, Y.-B. Li, Y. He, G. Xiao and F.-X. Xiao, *J.Phys. Chem. C*, 2019, **123**, 9721-9734.
2. S. Hou, Z.-Q. Wei, X.-C. Dai, M.-H. Huang and F.-X. Xiao, *Inorg. Chem.*, 2020, **59**, 7325-7334.
3. S. Hou, M.-H. Huang, Y.-B. Li, S. Xu, X. Lin, X.-Y. Fu and F.-X. Xiao, *Inorg. Chem.*, 2020, **59**, 16654-16664.
4. J.-Y. Li, Y.-H. Li, F. Zhang, Z.-R. Tang and Y.-J. Xu, *Appl. Catal. B-Environ.*, 2020, **269**, 118783.
5. Z.-Q. Wei, S. Hou, X. Lin, S. Xu, X.-C. Dai, Y.-H. Li, J.-Y. Li, F.-X. Xiao and Y.-J. Xu, *J. Am. Chem. Soc.*, 2020.
6. T. Li, Y.-B. Li, X.-C. Dai, M.-H. Huang, Y. He, G. Xiao and F.-X. Xiao, *J.Phys. Chem. C*, 2019, **123**, 4701-4714.
7. T. Hou, B. Wang, M. Ma, A. Feng, Z. Huang, Y. Zhang, Z. Jia, G. Tan, H. Cao and G. Wu, *Compos. Part B-Eng.*, 2020, **180**, 107577.
8. Z. J. Li, J. J. Wang, X. B. Li, X. B. Fan, Q. Y. Meng, K. Feng, B. Chen, C. H. Tung and L. Z. Wu, *Adv. Mater.*, 2013, **25**, 6613-6618.
9. H. Wang, R. Zhao, H. Hu, X. Fan, D. Zhang and D. Wang, *ACS Appl. Mater. Inter.*, 2020, **12**, 40176-40185.
10. L. Parrott and E. Erasmus, *RSC Adv.*, 2020, **10**, 32885-32896.
11. H.-J. Lin, Q.-L. Mo, S. Xu, Z.-Q. Wei, X.-Y. Fu, X. Lin and F.-X. Xiao, *J. Catal.*, 2020, **391**, 485-496.
12. X. Zhang, X. Hu, P. Guan, N. Zhang, J. Li and C. Du, *J. Mater. Sci.*, 2017, **52**, 4713-4726.